CIGRE-US National Committee
2020 Next Generation Network Paper Competition

Do FERC Orders Nos. 827 and 842 Usher in Grid Forming Control?

D. RAMASUBRAMANIAN
CIGRE Member ID: 120181405
Engineer/Scientist III
Electric Power Research Institute, Knoxville, TN
Professional with 10 years or less experience
dramasubramanian@epri.com

SUMMARY

FERC Orders Nos. 827 and 842 came into effect in 2016 and 2018 respectively. These orders, along with their regional amendments, mandate newly interconnecting inverter-based resources to have the capability to perform automatic voltage control and provide sustained primary frequency response. While there is no explicit requirement to compulsorily maintain capacity/energy headroom, this paper investigates if energy headroom is maintained, and if inverter controllers are as per these orders along with non-zero current injection during large disturbances, then would an all inverter island continue to operate in a stable manner upon being disconnected from the rest of the system. Provision of frequency response is through the presence of energy storage elements who also provide voltage control. All inverter-based resources in the system under study have phase locked loop control systems to track the angle of the grid voltage and maintain synchronism with the rest of the network. It will be shown in the paper that with proper conditioning of the active and reactive power reference commands, through controllers influenced by FERC Orders Nos. 827 and 842, even an inverter based resource with a phase locked loop can itself both form the grid and follow the grid at the same time. The performance of the control loops for a variation in size of the energy storage elements will also be discussed. Finally, the inherent speed of response that can be achieved from an inverter based resource will be leveraged to implement a dynamic domain interpretation of a distributed slack bus approach to enable quick power sharing across the inverters while also achieving fast and accurate control of electrical frequency within the system. The effectiveness and behaviour of this control in bringing the electrical frequency back to a nominal value within seconds after the occurrence of a load – generation mismatch event will be showcased even with the presence of a synchronous machine.

KEYWORDS

All inverter, FERC Orders Nos. 827 and 842, grid forming, primary frequency response

An increase in inverter-based resources (IBRs), or inverter-based generation (IBG), in the bulk power system has generated research and discussion around the viability of operation of an all inverter system. The reduction in the synchronous machine fleet, along with the fact of IBRs being located geographically far away from the transmission system, results in a reduction in the short circuit strength/stiffness of the system. This is both due to reduction in fault current availability at the point of interconnection bus of the IBR and due to the large physical impedance between the point of interconnection bus and the electric centre of the system. A reduction in system stiffness results in increased voltage sensitivity to change in current injections, both in magnitude and phase.

Conventional IBRs operate with an objective to inject maximum available active power under all system frequency conditions. In order to achieve this objective, the inverters in these plants rely on tracking the grid voltage magnitude and phase (usually through a phase locked loop (PLL)) at all instances in time. Presently, current injection from IBRs is generally governed from first principles as shown in Figure 1

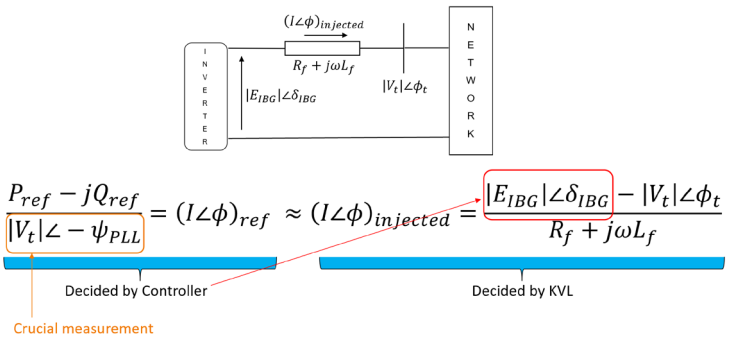

Figure 1
Obtaining current injected from conventional IBRs

Here, $|E_{IBG}|\angle\delta_{IBG}$ is the phasor representation of the sinusoidal voltage generated by the inverter (on its ac side), $|V_t|\angle\phi_t$ is the phasor representation of the voltage at the point of synchronization, and $R_f + j\omega L_f$ is the impedance between the inverter's ac side and the point of synchronization. The overall objective of the controls of an inverter is to ensure that $(I\angle\phi)_{injected}$ (whose value is influenced by Ohm's and Kirchhoff's Laws and thus influenced by the grid) is almost equal to $(I\angle\phi)_{ref}$. In order to meet this objective with a low time delay, $|V_t|\angle\phi_t$ should not be overly sensitive to change in current injections, while $\psi_{PLL} \approx \phi_t$ and $|E_{IBG}|\angle\delta_{IBG}$ should be defined as quickly as possible. Following this operation model, an inverter that can inject P_{ref} and Q_{ref} (often determined by a fixed power factor) successfully under varying grid conditions is said to follow the grid.

As the system approaches 100% inverters, and/or in local areas of the existing system with low short circuit strength, there is a possibility of increased sensitivity of $|V_t|\angle\phi_t$ to change in both in magnitude and phase of the injected current. It has been stipulated in research literature [1] that this high sensitivity of voltage can now result in inability of IBRs to operate in a stable manner as the PLL may be unable to track and lock onto the grid voltage (i.e. $\psi_{PLL} \neq \phi_t$), which will in turn result in inability to get $(I\angle\phi)_{ref} \approx (I\angle\phi)_{injected}$. Relaxing the need to get $(I\angle\phi)_{ref} \approx (I\angle\phi)_{injected}$ (i.e. bringing about an additional degree of freedom) is at the heart of so called grid forming inverter control topologies [1] which are proposed to be able to operate without a PLL or tracking the grid. This relaxation further brings about a relaxation in requiring $\psi_{PLL} \approx \phi_t$ as it allows for $|E_{IBG}|\angle\delta_{IBG}$ to be varied in a slower manner. It however brings about an increased uncertainty and variability in the amount of energy extracted from the dc side of the inverter as $(I\angle\phi)_{injected}$ is now not directly controlled unless it hits a limit. Handling this uncertainty in an IBR would also require the presence of an energy buffer in some form or manner, either with an additional energy storage component or with de-rated operation.

While there is a definite possibility of inverter control instability due to high sensitivity of voltage to change in current injection, it must be reasoned as to whether this instability is only due to the inability of the PLL to lock onto the voltage, or is it also in part due to the operation paradigm wherein the active power order does not change based on measured grid frequency? In order to meet Commission determinations in FERC Orders Nos.

827 and 842 [2, 3], inverters will now be required to include control loops that would change the active and reactive power references of an inverter with feedback based on grid conditions. The viability of operation of an all inverter system utilising these control loops, with closed loop settling time tuned to be few seconds allowing for continued operation of an all inverter system wherein the grid voltage is now naturally *formed* by all inverters with each inverter continuing to *follow* the rest of the system is discussed in this paper. Note that here the concept of black start and system restoration is not specifically discussed as it is a special operating condition even in a conventional power system.

It will be shown in this paper that under such a scenario a 100% IBR system, and an IBR system with 6% of the load served by synchronous machines (i.e. an approximate 94% IBR system), are stable for a variety of system disturbances and has robust fault ride through capability for both balanced and unbalanced faults. Further, the ability to share active power upon the occurrence of a disturbance, without violation of under frequency load shedding thresholds, will be shown. The active power sharing of the IBRs in the system will also introduce a new conceptual framework of using distributed slack bus *in a dynamic environment*. Using the concept of distributed slack bus, an all IBR system can share active power quickly upon the occurrence of a disturbance in order to bring the system frequency close to the nominal value. Such a response is possible through leveraging the nimble behaviour of inverters. To summarize, the contributions of this paper are: (1) Show the viability of robust and stable fault ride through behaviour of a system with large percentage of IBRs through implementation of FERC Orders Nos. 827 and 842, (2) Show adequate and quick sharing of power upon occurrence of a load or generation event, and (3) Introduce a concept of power sharing based upon distributed slack bus in the dynamic time frame.

IBR CONTROL STRUCTURE

In a conventional IBR resource, predominantly, a constant value of P_{ref} and Q_{ref} is used resulting in a rigid operating condition that could lead to instability with increase in percentage of IBRs. A generic representation of the control structure is shown in Figure 2. Here, P_{ref} is represented as P_{mppt} to designate the maximum power point reference.

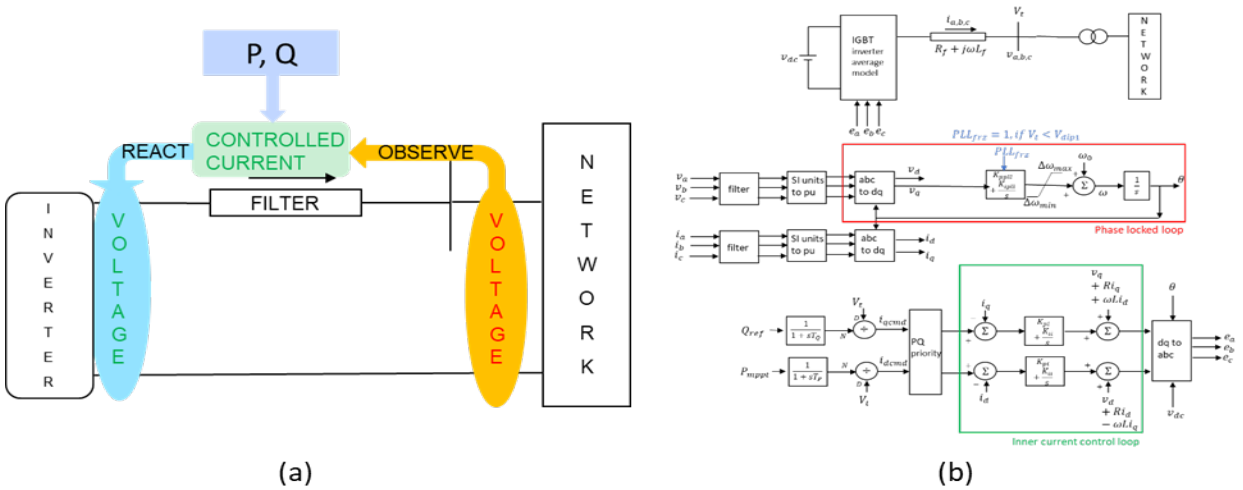

Figure 2
Structure of conventional IBR controllers at (a) functional high level, and (b) in generic detail

However, from control theory principles, a closed loop feedback system can be stabilized if the reference quantities are changed in an appropriate manner based on change in output of the control loop. Thus, using measured values of the network angle and voltage magnitude ($|V_t|\angle\psi_{PLL}$), the active power and reactive power references (P_{ref} and Q_{ref}) of the inverter controls can be modified with feedback based on grid conditions. Application of both FERC Orders Nos. 827 and 842 results in a modification of the evaluation of $(I\angle\phi)_{ref}$ wherein active power reference becomes a function of the voltage angle while reactive power reference becomes a function of voltage magnitude. Mathematically, this can be represented as,

$$\frac{P_{ref}\left(\Delta\psi_{PLL},\dot{\psi}_{PLL}\right)-jQ_{ref}(|V_t|)}{|V_t|\angle-\psi_{PLL}}=(I\angle\phi)_{ref}\approx(I\angle\phi)_{injected}=\frac{|E_{IBG}|\angle\delta_{IBG}-|V_t|\angle\phi_t}{R_f+j\omega L_f}$$

where now, active power reference is a function of PLL angle deviation ($\Delta\psi_{PLL}$) and rate of change of PLL angle ($\dot{\psi}_{PLL}$), while reactive power reference is a function of voltage magnitude at the point of synchronization ($|V_t|$). The specific implementation of these interdependencies for this paper is as shown in Figure 3. An additional power control loop is introduced which uses inputs from the PLL to define the change in active power reference while a voltage control loop is used to change the reactive power reference.

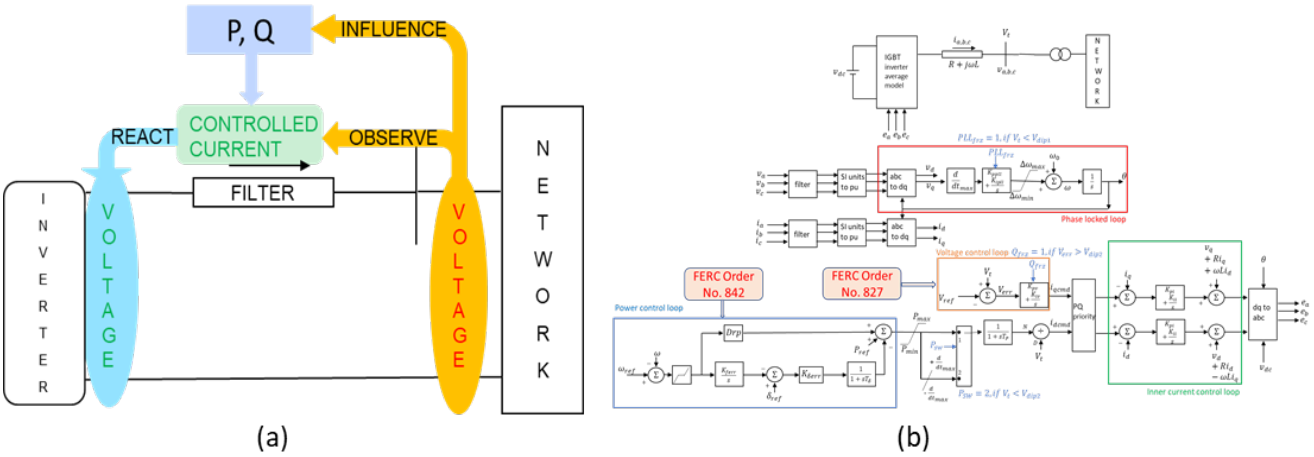

Figure 3
Structure of IBR controllers with FERC Orders Nos. 827 and 842 interdependencies included at (a) functional high level, and (b) in generic detail used in this paper

Inclusion of these interdependencies might at first seem trivial. However, to-date, very few bulk power system connected IBRs operate under such a fashion. Although the concept behind this form of control has been researched in islanded operation of microgrids [4,5], its applicability to the operation of an all inverter bulk power system has not been previously considered. In the subsequent section, simulation results using this control structure will be discussed to show the applicability and use in a transmission system.

SIMULATION RESULTS

The single line diagram of the system setup is shown in Figure 4 with simulations carried out in an electromagnetic transient (EMT) simulation program with a time step of 5µs. Each of the wind farms operate at a maximum power of 200 MW while controlling voltage at the MV side of the transformer. The wind farms are modelled using default models available from [6] (shown generally as in Figure 2). As they operate with a maximum power objective, additional battery energy storage is co-located at the point of interconnection to regulate the net active power output into the transmission network. The presence of the energy storage elements also brings in implementation of FERC Order No. 842. These energy storage elements, and the energy storage at Bus 6, have controllers as shown in Figure 3. It should be noted here that the size of the energy storage elements (200 MVA and 500 MVA respectively) are initially assumed to be a large value to show case the proof of concept behaviour of the control structure. Sensitivity analysis with reduction in size and location of the storage devices are discussed towards the end of the paper. Further, the energy storage at Bus 6 need not be a single large energy storage. It can rather itself be representative of an equivalenced all inverter island.

The green arrows in Figure 4 indicate the location of measurement of voltage, and direction of measured P and Q. The total pre-disturbance IBR generation level is 1.2 GW with a total load of 1.02 GW (constant current

active part and constant impedance reactive part). The entire 1.2 GW of IBR generation is assumed to be situated geographically and electrically far away from the load centres (as shown by the 100km long transmission lines). The system is started up with the equivalent source (at Bus 6) in service as the scope of this paper is not to address black start of an all inverter system. At *t=2s*, the breaker of the equivalent source is disconnected, thereby creating an all IBR system with 100% of the load served through IBRs and simultaneously introducing a load reduction (i.e. increased generation) of 180 MW (or 15% load rejection).

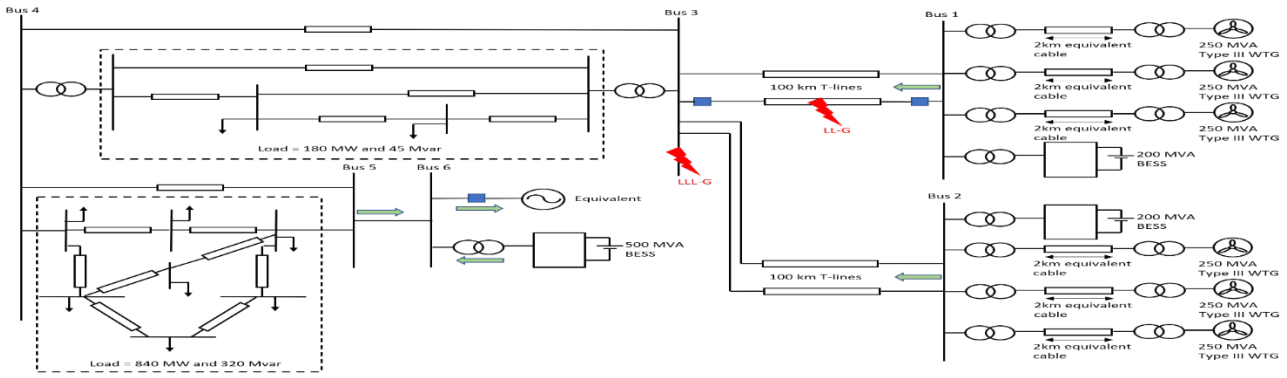

Figure 4
Single line diagram of system under study

To showcase a robust fault ride though behaviour, at *t=3s*, an 80ms solid three phase fault is applied on Bus 3. Further, at *t=5s*, an 80ms LL-G fault is applied at the centre of one of the transmission lines between Buses 1 and 3 followed by opening of the line at *t=5.2s*. Opening of the line following the fault introduces additional stress on the network by effectively doubling the impedance of the 100km power transfer path. The active power, reactive power, voltage magnitude, and current is shown in Figure 5. Due to participation in frequency control, on disconnection of equivalent source at *t=2s*, the surplus generation of around 180 MW is absorbed by the three energy storage sources (at Buses 1, 2, and 6) per action of their FERC Order No. 842 representative controller. Here, although the 'grid' is disconnected, due to the closed loop feedback control action of the control in conjunction with the PLL, the inverters both form the new grid and themselves follow the grid.

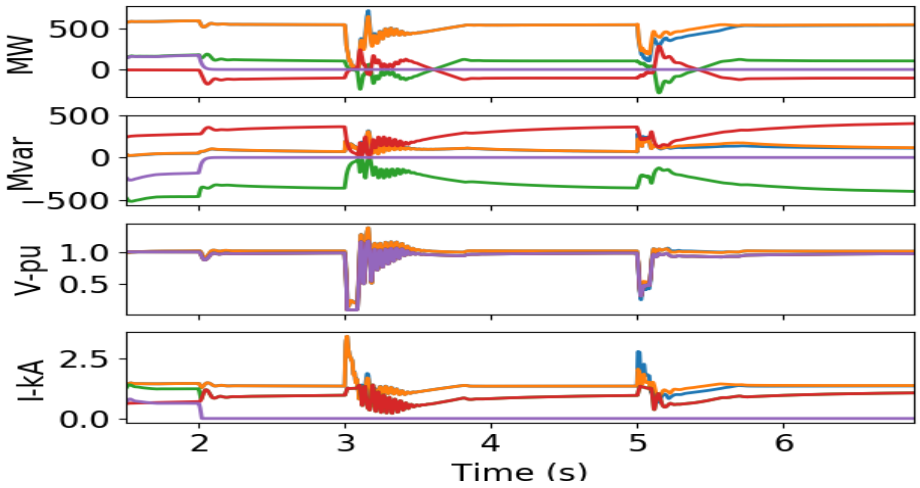

Figure 5
Performance of system for disconnect of equivalent source at t=2s and subsequent LLL-G and LL-G faults at t=3s and t=5s respectively (legend: Bus 1, Bus 2, Bus 5, 500 MVA BESS, Equivalent)

For the fault at Bus 3 at *t=3.0s*, both wind farm interconnections (measured at Bus 1 and Bus 2 respectively) contribute a maximum of 3kA on 230 kV while the short circuit current contribution from the 500 MVA energy storage is only around 1kA. The fault ride through and recovery is within conventional performance criteria.

This is despite the extremely low short circuit current contribution to the fault. This operating paradigm with controllers representative of FERC Orders Nos 827 and 842 is thus possibly a viable operating paradigm.

The response at Bus 1 for an increase in load following the disconnection of the equivalent source is shown in Figure 6. The load in the subsystem between Bus 3 and Bus 4 is increased by 120 MW/30 Mvar at *t=3s* (around 11% increase in load). A droop gain of 20.0 (5% droop) is recommended in FERC Order No. 842. The behaviour of the system for two values of droop gain, 20.0 and 2.0, is shown in the plot. The larger value of gain (as per FERC Order No. 842 recommendation) leads to a more robust system behaviour within acceptable criteria.

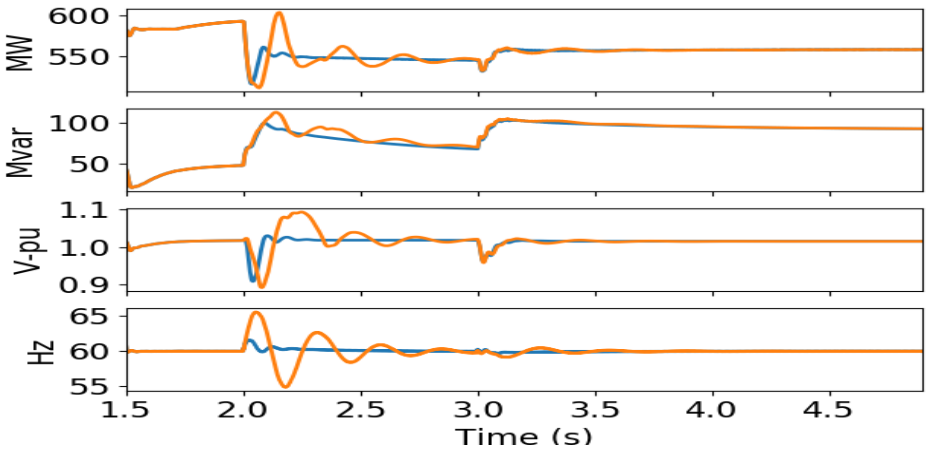

Figure 6
Behaviour at Bus 1 for disconnect of equivalent source at t=2s and subsequent load increase of 120 MW/30 Mvar at t=3s (legend: Droop gain of 20, Droop gain of 2.0)

At this juncture, a commentary on the active power sharing scheme employed by the three energy storage elements is warranted. As mentioned before, in this scenario, the Type III wind turbines operate at their maximum power point and thus do not have the capability to modulate their active power output in relation to frequency change. However, for the energy storage elements, a dynamic domain variation of a distributed slack bus is implemented to supplement the operation of a conventional frequency based droop control. When solving a distributed slack bus power flow problem, rather than allocating the power mismatch (generation – load) to a single slack generator, the mismatch is distributed amongst every generator in the system. The percentage of the mismatch allocated to each generator is proportional to the losses in the network [7] which is a function of bus voltage angle at the generator bus between two iterations of the power flow solution. Extending this concept to the dynamic domain, the equation for the power reference command can be written as:

$$P = P_{ref} + K_{\delta err}\left(\delta_{ref} - \int K_{ferr}\left(1.0 - \dot{\hat{\theta}}\right)dt\right) + Drp\left(1.0 - \dot{\hat{\theta}}\right).$$

Here, $K_{\delta err}\left(\delta_{ref} - \int K_{ferr}\left(1.0 - \dot{\hat{\theta}}\right)dt\right)$ represents the component which is the dynamic domain equivalent of the distributed slack bus concept wherein the active power command is varied in proportion to the change in bus voltage angle. Incidentally, this component also enables achieving tight control on electrical frequency resulting in frequency returning to nominal value within few seconds of the disturbance.

The presence of a 200 MVA storage system co-located with a 750 MVA IBR plant stretches the realm of a practical study. To make the scenario reflective of a possible practical system, the presence of distributed smaller energy storage devices rather than large energy storage elements co-located with the wind farms was studied. For this, instead of two 200 MVA energy storage at the wind farms, seven 50 MVA energy storage devices were placed within the subsystem between Bus 4 and Bus 5. One energy storage device was placed at each of buses within the subsystem with local terminal voltage control. The response observed at the 500 MVA energy

storage at Bus 6 for the disconnection of the equivalent source at *t=2s* followed by the increase in load in the subsystem between Bus 3 and Bus 4 is shown in Figure 7. The response is compared to the scenario discussed previously with the large energy storage (two 200 MVA BESS) with droop gain of 20. The distributed BESS also contribute to the frequency response.

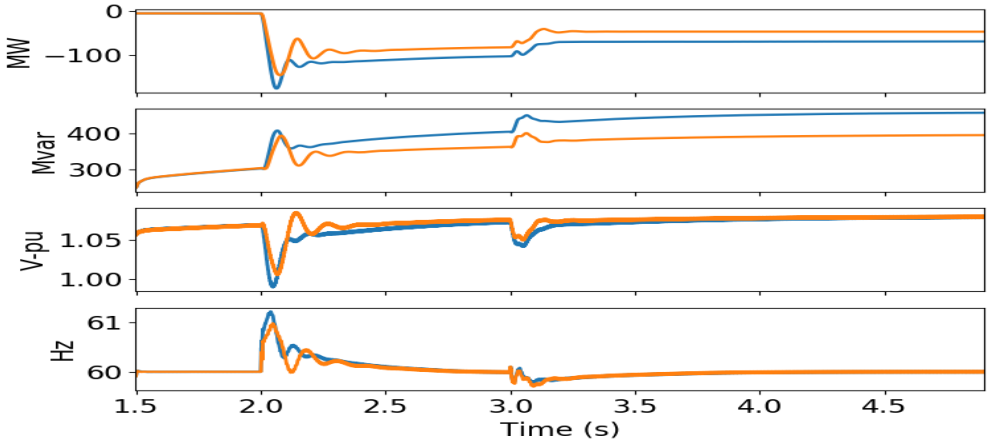

Figure 7
Behaviour at Bus 6 for disconnect of equivalent source at t=2s and subsequent load increase of 120 MW/30 Mvar with distributed energy storage (legend: Large two 200 MVA energy storage, Small seven 50 MVA energy storage)

As expected, with more distributed frequency control, the dynamic response of the system is marginally improved. However here it must be mentioned that due to the lack of sufficient active power control from the wind farms, the system was unable to ride through the fault and subsequent opening of the line between Bus 1 and Bus 3. It was however able to ride through the fault at Bus 3.

In the above scenario, since Type III wind turbines were used, an argument can be made that the system is not a pure 100% IBR system. Thus, to further investigate the sensitivity of system performance with IBR resource type and with respect to the size of energy storage, few modifications as listed below were made to the system shown previously in Figure 4:

1. All Type III wind turbine plants (including the 2km cable) were replaced with a representative electrical model of a solar or Type IV plant with a controller structure that did not include representation of FERC Order No. 842 but included representation of FERC Order No. 827.
2. The size of the two 200 MVA energy storage elements were reduced to 20 MVA each.
3. The size of the 500 MVA energy storage element was reduced to 150 MVA and its location was moved from Bus 6 to Bus 4 to provide improved voltage support.
4. The equivalent source at Bus 6 was replaced with a 250 MVA synchronous machine with a hydro turbine dispatched at around 90 MW
5. The loading level in the system increased by 150 MW

With these changes, 94% of the load is served by IBR thereby making the system under study similar to a realistic and practical system. In addition, the lower size of the energy storage elements also helps illustrate the viability of the controller topology influence by FERC Orders Nos. 827 and 842. Figure 8 shows the voltage magnitude and active power injection observed in this modified system for successive LL-G (and subsequent opening of the line) applied at *t=5.0s* on the transmission line between Bus 1 and Bus 3, and LLL-G fault applied at *t=7.0s* on Bus 3.

In this scenario, the voltage at Bus 1 following the clearance of the LLL-G at Bus 3 (*t=7.1s*) is important to note. Upon fault clearance, the voltage magnitude at Bus 1 shows a phenomenon that is similar to the beginning of a voltage collapse wherein the voltage reduces when the fault clears (shown in the figure inset). The reduction

in the MVA ratings of the energy storage devices reduced the overall voltage and frequency support available in the system. Further, the 250 MVA IBRs (Type III WTG or Type IV/Solar) have a slow ramp rate of recovery of active power (2.5pu/s in this case) as following clearance of a fault in a weak grid, it may not be advisable to quickly ramp power injection through a long transmission line [8]. Thus here, the need to have slower active power injection to maintain system stability coupled with the lower amount of voltage support from the reduced ratings of the energy storage plants causes a deficit in reactive power which results in a near voltage collapse.

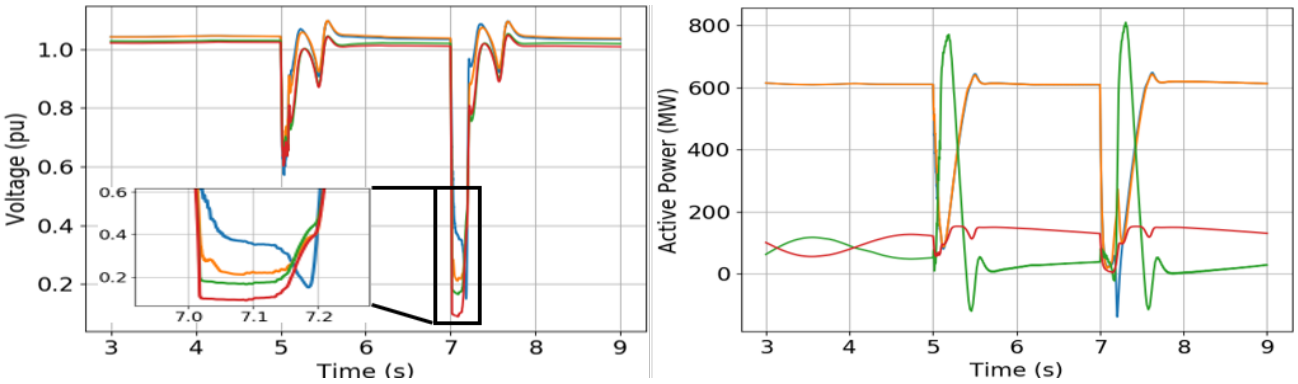

Figure 8
Voltage magnitude and active power for a LL-G applied at t=5.0s and LLL-G fault applied at t=7.0s with reduced size of energy storage elements (legend: Bus 1, Bus 2, Bus 5, Bus 4)

The impact of size of the storage devices on the frequency response of the system is shown in Figure 9 for a 10% load increase at *t=1.5s*. Here, four scenarios are considered: (1) Scenario 1: distributed slack bus based control with 150 MVA energy storage at Bus 4 and 20 MVA each at Bus 1 and Bus 2, (2) Scenario 2: conventional 5% frequency droop control with same storage size as Scenario 1, (3) Scenario 3: distributed slack bus based control with 150 MVA energy storage at Bus 4 and 100 MVA each at Bus 1 and Bus 2, (4) Scenario 4: conventional 5% frequency droop control with same storage size as Scenario 3. Right away it can be seen that with conventional droop based frequency control, while there is an improvement in the frequency response with the 100 MVA storage at Buses 1 and 2, the frequency nadir is below the UFLS threshold. However, with the distributed slack bus based frequency control, the response in Scenarios 1 and 3 are superior to the response with conventional frequency droop control. Additionally, with the larger size of storage at Buses 1 and 2, the nadir is above the UFLS threshold and the frequency settles back to the nominal value within few seconds. The active power output at Bus 1 and Bus 4 is also shown for the four scenarios. Note that in these simulations, the controllers are not tuned to deliver an optimal response as the objective is to show a proof of concept.

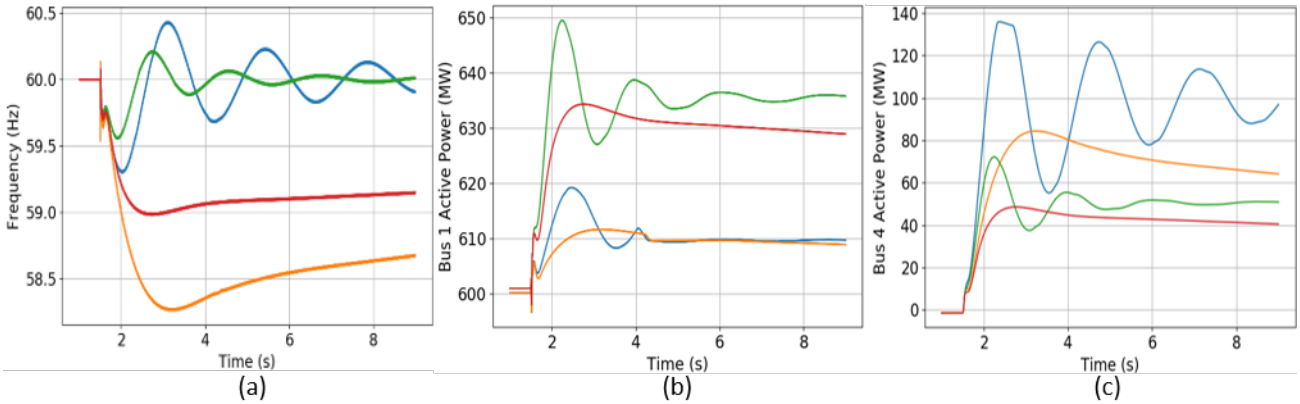

Figure 9
For a 10% load increase (a) electrical frequency, (b) active power at Bus 1, (c) active power at Bus 4 (legend: Scenario 1, Scenario 2, Scenario 3, Scenario 4)

CONCLUSION

The scenarios shown in this paper serve to validate the initial hypothesis that possibly an all inverter system (or a system with large instantaneous penetration of inverters) can be operationally viable with conventional form of active power-frequency and reactive power-voltage controls along the lines of the concepts laid out in the two recent FERC Orders Nos. 827 and 842. While the response and behaviour might seem intuitive and trivial, they hold extreme significance in today's changing power system. With this framework, it is possible for IBRs to provide essential reliability services that are necessary for reliable grid operation, without needing to mimic/virtualize synchronous machines. Here, the interdependence between IBR control behaviour and protection system behaviour is not discussed but is a topic of future research. Further, the notion of grid following and grid forming could possibly be merged as they represent the cause and effect of closed loop feedback control in an interconnected system. It goes without saying that requiring adequate capacity/energy headroom with sufficient speed of delivery upon the occurrence of a disturbance is crucial. However, this is a basic tenet to obtain a reliable operation of any interconnected power system and not just one with IBRs.

Every form of closed loop control has its own region of stability and applicability which needs to be considered for stable and reliable system operation. Further, with IBRs replacing synchronous machines, not only does the short circuit strength in the system reduce, but potentially so does the available reactive power support. As shown in the scenario with the reduced MVA ratings for energy storage elements, the behaviour of the power system follows fundamental electrical systems theory and the behaviour of the control system is a consequent impact.

Through the ratification of FERC Orders Nos. 827 and 842, power systems may already be on their way to bringing in “grid-forming” capability by exploring the possibility of IBRs operating flexibly in relation to grid conditions, rather than be rigid power/current injection devices. As with any new concept, optimism must be balanced with caution. System reliability and stability should not depend upon just one new solution, but rather a multitude of complementary solutions, both from generation planning and transmission planning.

BIBLIOGRAPHY

[1] G. Denis, “The MIGRATE Project: The Challenges of Operating a Transmission Grid with only Inverter-Based Resources. A Grid Forming Control Improvement with Transient Current-Limiting Control,” *IET Renewable Power Generation*, vol. 12, pp. 523-529(6), Apr. 2018.

[2] Federal Energy Regulatory Commission, “Reactive Power Requirements for Non-Synchronous Generation,” *Docket No. RM16-1-000, Order No. 827*, Jun. 2016 [Online: https://www.ferc.gov/whats-new/comm-meet/2016/061616/E-1.pdf]

[3] Federal Energy Regulatory Commission, “Essential Reliability Services and the Evolving Bulk-Power System – Primary Frequency Response,” *Docket No. RM16-6-000, Order No. 842*, Feb. 2018 [Online: https://www.ferc.gov/whats-new/comm-meet/2018/021518/E-2.pdf]

[4] M. Surprenant, I. Hiskens, and G. Venkataramanan, “Phase Locked Loop Control of Inverters in a Microgrid,” in *2011 IEEE Energy Conversion Congress and Exposition*, Sep. 2011, pp. 667-672

[5] M. Yazdanian and A. Mehrizi-Sani, “Washout filter-based power sharing,” *IEEE Transactions on Smart Grid*, vol. 7, no. 2, pp. 967–968, Mar. 2016.

[6] Manitoba Hydro International Ltd. (MHI), “Type 3 Wind Turbine Generators (WTG) (for PSCAD v4.6),” PSCAD Knowledge Base, Nov. 2018 [Online: https://www.pscad.com/knowledge-base/article/496]

[7] P. H. Haley and M. Ayres, “Super Decoupled Loadflow With Distributed Slack Bus,” *IEEE Transactions on Power Apparatus and Systems*, vol. PAS-104, no. 1, pp. 104-113, Jan. 1985

[8] H. Ma and J. Nielsen, “Siemens Wind Turbine Weak Grid Option Modeling in PSSE WECC library”, WECC Modeling and Validation Work Group (MVWG), Mar. 2017